

Reconstructing $\delta^{13}\text{C}$ isoscapes of phytoplankton production in a coastal upwelling system with amino acid isotope values of littoral mussels

Natasha L. Vokshoori^{1,*}, Thomas Larsen², Matthew D. McCarthy^{1,*}

¹University of California, Santa Cruz, Ocean Sciences Department, 1156 High Street, Santa Cruz, California 95060, USA

²Christian-Albrechts University of Kiel, Leibniz-Laboratory for Radiometric Dating and Stable Isotope Research, Max-Eyth-Str. 11-13, 24118 Kiel, Germany

ABSTRACT: Compound-specific isotope analysis of amino acids (CSI-AA) is increasingly used to decouple trophic isotopic effects from isotopic composition at the base of food webs. The $\delta^{13}\text{C}$ values of essential amino acids (EAAs) are particularly useful as recorders of primary production, because animals cannot synthesize EAAs de novo, so diagnostic biosynthetic $\delta^{13}\text{C}_{\text{EAA}}$ patterns remain unchanged up food chains. To test the potential for $\delta^{13}\text{C}_{\text{AA}}$ values to identify C source and resource flow in complex littoral ecosystems, we measured bulk and $\delta^{13}\text{C}_{\text{AA}}$ values of *Mytilus californianus* adductor muscle tissue in samples spanning >1700 km of coastline from San Diego, California, to southern Oregon, USA. The average bulk $\delta^{13}\text{C}$ value for the entire region clustered around a relatively constant value ($-15.7 \pm 0.9\text{‰}$), with no latitudinal trend ($R^2 = 0.022$). $\delta^{13}\text{C}_{\text{AA}}$ patterns were highly consistent in all mussels, and $\delta^{13}\text{C}_{\text{EAA}}$ patterns closely matched expectations for marine phytoplankton, supporting the hypothesis that consumer EAA isotope values are unchanged from primary production. While bulk $\delta^{13}\text{C}$ values were ambiguous in terms of source, application of a multivariate $\delta^{13}\text{C}_{\text{EAA}}$ 'fingerprinting' approach clearly indicated microalgae as the major source for all mussel EAAs. We hypothesize that integrated $\delta^{13}\text{C}$ values of coastal phytoplankton production can therefore be directly derived from $\delta^{13}\text{C}_{\text{EAA}}$ of filter feeders in coastal regions. A correction derived from literature data for phytoplankton $\delta^{13}\text{C}_{\text{EAA}}$ values yielded reasonable $\delta^{13}\text{C}$ values for coastal production, supporting this idea. Together, our results suggest $\delta^{13}\text{C}_{\text{EAA}}$ as a new approach for constructing baseline $\delta^{13}\text{C}$ isoscapes and may have important implications for ecosystem studies in both modern and paleo-environments.

KEY WORDS: *Mytilus californianus* · Carbon isotopes · Compound-specific isotope analysis · California · Isoscape

Resale or republication not permitted without written consent of the publisher

INTRODUCTION

Ecological studies have increasingly used stable isotope values of carbon (C) in organisms, detrital organic matter, and fossils to estimate trophic position, study food web linkages, and understand basic biogeochemical cycling (Burton et al. 1999, Sherwood et al. 2005, Newsome et al. 2007, Ruiz-Cooley & Gerrodette 2012). Due to variation in both biosynthetic pathways and CO_2 uptake mechanisms, $\delta^{13}\text{C}$

values can be useful for differentiating between major C sources in the marine environment. These include not only major potential endmember sources of organic matter such as terrestrial plants, marine micro algae, coastal macrophytes, or chemosynthetic production (Altabet 1996), but similar sources from different ocean regions (Rau et al. 1990, 1992, 2001, Goericke & Fry 1994).

Over broad spatial scales, maps of variation in baseline isotope values versus ocean region are

*Corresponding authors: nvoksho@ucsc.edu;
mdmccar@ucsc.edu

termed 'isoscapes,' and they represent a growing approach for identifying major ocean biogeochemical zones (Graham et al. 2010, Hobson et al. 2010, Somes et al. 2010, McMahon et al. 2013). Accurate isoscapes not only provide a quantitative mapping of major biogeochemical provinces on an ecosystem-wide scale, but they can also be used to understand animal migration or trophic connections through isotope values measured in specific organisms (Hansson et al. 1997, Aurioules et al. 2006, Newsome et al. 2007).

However, all of these applications also have a number of inherent drawbacks in the common use of bulk $\delta^{13}\text{C}$ isotope values. First, trophic transfers impart a variable, and relatively poorly constrained isotope fractionation for bulk $\delta^{13}\text{C}$ values. While trophic enrichment factors (TEFs) for bulk $\delta^{13}\text{C}$ values are often assumed to be relatively small (0.5–1‰; e.g. Fry & Sherr 1984, Peterson & Fry 1987), more recent studies have shown that bulk $\delta^{13}\text{C}$ values can in fact be highly variable (–3 to +4‰), depending on food quality and the tissue type analyzed (Post 2002). Further, differing environmental growth conditions can also result in very different bulk $\delta^{13}\text{C}$ values, even for the same primary producers. For example, temperature and possibly salinity are physical parameters that are known to control ^{13}C fractionation in ocean algae (Rau et al. 1992, Barnes et al. 2009), and in coastal macrophyte species both growth depth and seasonal period correspond with very large, characteristic variations in $\delta^{13}\text{C}$ values (e.g. Simenstad et al. 1993, Kaehler et al. 2006, Page et al. 2008, Tallis 2009, Foley & Koch 2010). Such changes can greatly complicate attempts to use bulk isotopes to understand specific C sources and resource flows and can be particularly problematic for producing representative isoscapes from necessarily limited sampling.

The need to integrate such seasonal and environmental variation is one reason that isoscapes are often constructed from measurements made on consumers of well-known residency and diet (Olson et al. 2010, McMahon et al. 2013). Filter-feeding mollusks, such as mussels, are excellent candidates in this regard, as they are sessile animals which continuously integrate isotopic signatures of local suspended particulate food sources. Therefore, bulk $\delta^{13}\text{C}$ values at a given site should reflect the relative distribution of major food sources. However, for the reasons noted above, measured bulk isotope $\delta^{13}\text{C}$ values can be significantly decoupled from original primary production values, and it is also often very difficult to identify major sources with any confidence. This is a particular problem in productive littoral systems,

where potential C sources are typically numerous and complex, often consisting of both marine and terrestrial endmembers (Cloern et al. 2002, Larsen et al. 2012).

Compound-specific isotope analysis of amino acids (CSI-AA) is a rapidly developing tool that can directly address many inherent issues with bulk isotope data. CSI-AA work to date suggests that $\delta^{13}\text{C}$ AA patterns ($\delta^{13}\text{C}_{\text{AA}}$) show great promise as a specific tracer for C sources in food webs (e.g. McMahon et al. 2011, Larsen et al. 2012) that can at the same time remove uncertainty related to TEF values and trophic transfer. The $\delta^{13}\text{C}$ of the non-essential AAs ($\delta^{13}\text{C}_{\text{NAA}}$), which have carbon skeletons that can be synthesized de novo by animals, have been used to infer detailed information about the isotopic routing of a consumer's diet. In contrast, $\delta^{13}\text{C}$ values of the essential AAs ($\delta^{13}\text{C}_{\text{EAA}}$; phrasing consistent with Larsen et al. 2009) are preserved unchanged up food chains because most animals cannot synthesize these C skeletons (O'Brien et al. 2002, Fogel & Tuross 2003, Howland et al. 2003, Jim et al. 2006, McMahon et al. 2010, Newsome et al. 2011). This means that $\delta^{13}\text{C}_{\text{EAA}}$ relative to bulk or $\delta^{13}\text{C}_{\text{NAA}}$ values can potentially be used to decouple $\delta^{13}\text{C}$ values of baseline sources (i.e. primary production) from heterotrophic fractionation. Moreover, recent research has demonstrated that $\delta^{13}\text{C}_{\text{EAA}}$ patterns are diagnostic of phylogenetic C sources (Larsen et al. 2009, 2013) and trace C flow in ecosystems (McMahon et al. 2011). Together, these aspects suggest great promise for $\delta^{13}\text{C}_{\text{EAA}}$ to track C sources and baseline primary production $\delta^{13}\text{C}$ values through marine food webs and to create truly integrated isoscapes of primary production $\delta^{13}\text{C}$ values.

Here we examined for the first time $\delta^{13}\text{C}_{\text{AA}}$ patterns in littoral mussels, sampled over a wide geographic range along the California (USA) coast. We sampled mussels across 10 degrees of latitude in the coastal zone of the California Upwelling Ecosystem (CUE). The major goals of our study were as follows: first, to compare EAA vs. NAA $\delta^{13}\text{C}$ patterns between mussels and primary producers to test the basic hypothesis that $\delta^{13}\text{C}$ values of EAAs in mussel tissue should represent a direct isotopic record of composite source primary production. Second, because the CUE is a dynamic system with multiple possible food web C sources, we also tested a CSI-AA 'fingerprinting' approach to assess whether major C sources can be directly identified by CSI-AA, in the face of ambiguous bulk $\delta^{13}\text{C}$ data. Finally, we used literature data on phytoplankton $\delta^{13}\text{C}_{\text{EAA}}$ patterns to propose a proxy for direct estimation of $\delta^{13}\text{C}$ of primary production

from $\delta^{13}\text{C}_{\text{EAA}}$ in heterotrophs. Our overarching hypothesis is that by measuring $\delta^{13}\text{C}_{\text{EAA}}$ in long-lived organisms (i.e. mussels), it will ultimately be possible to directly estimate integrated values for $\delta^{13}\text{C}$ of local primary production.

MATERIALS AND METHODS

Sample collection and preparation

California mussels *Mytilus californianus* were collected from 28 different sites between Coos Bay, Oregon (OR), and San Diego, California (CA), in the winter of 2009/2010 (Table 1). Sites were chosen to be approximately evenly distributed along the CA coastline, with ~80 km geographic separation. Typically 5 mussels were collected from each site, all between 30 and 40 mm maximum shell length, and

were immediately placed on dry ice until further preparation. The adductor muscle of each individual was dissected for analysis. This tissue was selected because the isotopic value of adductor tissue in this size class of mussel is considered to have a long turnover time (Gorokhova & Hansson 1999). Therefore, these samples should integrate approximately annual variability in suspended food source isotopic values. The adductor tissue was carefully dissected from all other tissues, rinsed with deionized water, refrozen, and then freeze-dried. Lipids were removed following the methods of Dobush et al. (1985), using petroleum ether in a Dionex Accelerated Solvent Extractor. Finally, in preparation for CSI-AA, composite samples were made for 11 collection sites: 1 ± 0.05 mg of lyophilized tissue was weighed and combined for each individual mussel ($n = 5$). Further CSI-AA preparation proceeded as described below.

Table 1. *Mytilus californianus*. Collection site information and mean bulk $\delta^{13}\text{C}$ values. $\delta^{13}\text{C}$ values represent average values from 5 individual mussels in a narrow size range (see 'Materials and methods') taken from each site \pm SD

Site (USA)	Identifier	Habitat type	Latitude ($^{\circ}\text{N}$)	Longitude ($^{\circ}\text{W}$)	$\delta^{13}\text{C}$	SD
Humbug Mtn./ Port Orford, OR	HMPO	Rocky	42° 43'	124° 27'	-16.3	0.2
Meyer's Creek Beach, OR	MCPR	Rocky	42° 18'	124° 24'	-16.5	0.1
Pelican State Beach, CA	PSB	Rocky	41° 59'	124° 12'	-16.0	0.1
Lagoon Creek, CA	LC	Rocky	41° 36'	124° 06'	-15.9	0.1
Humboldt Lagoon, CA	HL	Rocky	41° 15'	124° 05'	-15.9	0.1
Luffenholtz Beach, CA	LB	Rocky	41° 02'	124° 07'	-16.1	0.4
Point Cabrillo Light-house, CA	PCL	Rocky	41° 02'	123° 49'	-17.3	0.3
Schooner Gulch, CA	SG	Rocky	41° 02'	123° 39'	-15.7	0.2
Stillwater Cove Marine, CA	SWC	Rocky	41° 02'	123° 17'	-14.5	0.1
Bodega Bay, CA	BB	Rocky	41° 02'	123° 4'	-15.1	0.2
Pacifica, CA	PAC	Rocky	41° 02'	122° 29'	-15.3	0.1
Half Moon Bay, CA	HMB	Jetty	41° 02'	122° 28'	-15.7	0.1
Davenport, CA	DAV	Rocky	41° 02'	122° 11'	-16.3	0.2
Santa Cruz, CA	SC	Rocky	41° 02'	122° 03'	-13.5	0.9
Moss Landing, CA	ML	Jetty	41° 02'	121° 47'	-13.9	0.9
Asilomar, CA	ASI	Rocky	41° 02'	121° 56'	-16.0	0.1
Rocky Point, CA	RP	Rocky	41° 02'	121° 54'	-16.5	0.5
Mill Creek, CA	MC	Rocky	41° 02'	121° 29'	-15.6	0.4
Morro Bay, CA	MB	Rocky	41° 02'	120° 52'	-15.5	0.3
Gaviota, CA	GAV	Rocky	41° 02'	120° 12'	-14.9	0.3
Santa Barbara, CA	SB	Rocky	41° 02'	119° 42'	-14.4	0.8
Ventura, CA	VEN	Jetty	41° 02'	119° 16'	-15.8	0.1
Malibu, CA	MAL	Rocky	41° 02'	118° 48'	-16.1	0.2
Topanga, CA	TOP	Rocky	41° 02'	118° 34'	-16.2	0.1
Venice Beach, CA	VB	Jetty	41° 02'	118° 28'	-15.2	0.6
San Clemente, CA	SCL	Pier	41° 02'	117° 37'	-17.3	0.5
Oceanside, CA	OCE	Jetty	41° 02'	117° 22'	-16.7	0.4
La Jolla, CA	LAJ	Rocky	41° 02'	117° 15'	-15.1	0.4

Bulk $\delta^{13}\text{C}$ analysis

Stable C isotope analyses were conducted using standard protocols in the Stable Isotope Lab at the University of California, Santa Cruz (UCSC-SIL; <http://es.ucsc.edu/~silab/index.php>). Briefly, homogenized muscle tissue of each individual was weighed into tin capsules and combusted. Isotope values were determined on a Carlo Erba 1108 elemental analyzer coupled to a Thermo Finnigan Delta Plus XP isotope ratio mass spectrometer (EA-IRMS). Analytical error associated with this measurement was typically $< \pm 0.15$. Stable isotopes are reported using standard delta (δ) notation in parts per thousand (‰):

$$\delta^{13}\text{C} = [(R_{\text{sample}}/R_{\text{standard}}) - 1] \times 1000 \quad (1)$$

where R is the ratio of heavy to light isotope, R_{sample} is from the sample, and the R_{standard} is Vienna PeeDee Belemnite (PDB) for C, as provided by pulses of calibrated CO_2 reference gas. For details on standard correction calculations, refer to the UCSC-SIL website above.

Compound-specific stable C isotope analysis

Individual AA $\delta^{13}\text{C}$ values were measured as trifluoroacetyl isopropyl ester (TFA-IP) AA derivatives, after acid hydrolysis. Samples were hydrolyzed by adding 2.5 mg homogenized composite muscle tissue to 1 ml of 6 N HCl, and heating for 20 h at 110°C under nitrogen. After drying, AA isopropyl esters were prepared with a 1:5 mixture of AcCl:2-propanol (110°C, 60 min) and then acylated using a 1:3 mixture of dichloromethane (DCM) and trifluoroacetic anhydride (TFAA) (100°C, 15 min). Derivatized AAs were dissolved in DCM to a final ratio of approximately 2.5 mg of original tissue to 250 μl DCM for injection on the gas chromatograph IRMS (GC-IRMS) system.

Isotopic analysis was conducted on a Thermo Trace GC Ultra with inline oxidation and reduction furnaces, coupled to a Thermo Finnigan Delta Plus XP IRMS, equipped with a CTC Analytics autosampler. Derivatives (1 μl) were injected (250°C constant temperature) onto an Agilent DB-5 column (50 m \times 0.32 mm ID \times 0.52 μm film thickness), with a He carrier flow rate of 2 ml min^{-1} (constant flow). Separations were achieved with a 4-ramp oven program: 52°C, 2 min hold; ramp 1 = 15°C min^{-1} to 75°C, hold for 2 min; ramp 2 = 4°C min^{-1} to 185°C, hold for 2 min; ramp 3 = 4°C min^{-1} to 200°C; ramp 4 = 30°C min^{-1} to 240°C, hold for 5 min. This method allowed for $\delta^{13}\text{C}$ determination of the following AAs in mussel tissue: non-essential AAs alanine (Ala), aspartic acid + asparagine (Asp), glutamic acid + glutamine (Glu), glycine (Gly), proline (Pro), serine (Ser), and tyrosine (Tyr); and essential AAs leucine (Leu), isoleucine (Ile), valine (Val), phenylalanine (Phe), and threonine (Thr). Acid hydrolysis destroys tryptophan and cysteine, so these were not detected, and it also deaminates asparagine to aspartic acid, and glutamine to glutamic acid. While the abbreviations Glx and Asx are sometimes used to denote the combined Gln+Glu and Asn+Asp peaks, in order to correspond better with extant CSI-AA literature, we have elected to simply use Asp and Glu abbreviations, as defined above.

All samples were analyzed on the GC-IRMS in triplicate, and measured AA $\delta^{13}\text{C}$ values were corrected for the C added during derivatization, following the approach of Silfer et al. (1991). Reproducibility for tissue samples was typically less than <0.3‰ (n = 3). The average mean deviation for all tissue sample replicates was 0.4‰.

Adductor muscle tissue AA molar percentages (mol %) values were determined from underivatized mussel hydrolysates, using an established high pres-

sure liquid chromatography - evaporative light scattering detector (HPLC-ELSD) technique (Broek et al. 2013).

Statistical analysis and calculations

To assess similarities of $\delta^{13}\text{C}_{\text{AA}}$ patterns between different samples, we normalized $\delta^{13}\text{C}$ values of each measured AA to the mean value of all EAAs in the sample:

$$\delta^{13}\text{C}_n = \delta^{13}\text{C}_{\text{AA-measured}} - \delta^{13}\text{C}_{\text{EAA-avg}} \quad (2)$$

where $\delta^{13}\text{C}_n$ is the normalized value for a given AA, $\delta^{13}\text{C}_{\text{AA-measured}}$ is the measured value, and $\delta^{13}\text{C}_{\text{EAA-avg}}$ is the average value of all EAAs within the same sample. This normalization approach allows direct assessment of biosynthetic signatures (i.e. $\delta^{13}\text{C}_{\text{AA}}$ patterns) by removing any variability associated with changes in baseline $\delta^{13}\text{C}$ between samples.

To predict the phylogenetic origins of essential AAs in mussel tissue, we applied the linear discriminant function analysis (LDA) approach of Larsen et al. (2009, 2012, 2013). Termed ' $\delta^{13}\text{C}_{\text{EAA}}$ fingerprinting' (Larsen et al. 2009), this approach uses LDA coupled with a 'training set' of $\delta^{13}\text{C}_{\text{EAA}}$ data from evolutionarily distinct groups of potential primary producers, in order to predict likely group membership based on measured $\delta^{13}\text{C}_{\text{EAA}}$ values. Our analysis used previously published training set data for 3 main potential C sources: eukaryotic marine microalgae, axenically cultured bacteria (as a proxy for detrital material), and brown macroalgae (Phaeophyceae) (Larsen et al. 2013) to predict group membership (Table S1; for inter-laboratory calibration of $\delta^{13}\text{C}$ values and trace outputs for LDA, see also Tables S3–S8 and Fig. S1 in the Supplement at www.int-res.com/articles/suppl/m504p059_supp.pdf). The analyses were performed in R version 2.12.1 (R Development Core Team 2012) using RStudio interface version 0.96.330 and R package MASS (Venables & Ripley 2002). We used Pillai's trace (multivariate ANOVA) to test the null hypothesis of no difference in classification between the groups. All other statistical analyses (e.g. hierarchical cluster analysis and *t*-tests) were conducted using the JMP statistical software package (SAS Version 10).

Finally, we propose a correction to derive $\delta^{13}\text{C}$ values of average source primary production based on $\delta^{13}\text{C}_{\text{EAA}}$ measured in *Mytilus californianus*, coupled with available data for $\delta^{13}\text{C}_{\text{EAA}}$ patterns in eukaryotic marine phytoplankton. While coupled bulk $\delta^{13}\text{C}$ and $\delta^{13}\text{C}_{\text{EAA}}$ plankton data are not yet extensive, we

compiled several datasets to observe the correlation across diverse cultured and environmental algal samples (see Table S2 in the Supplement). We used a regression approach between bulk $\delta^{13}\text{C}$ of total plankton biomass samples and the averaged $\delta^{13}\text{C}_{\text{EAA}}$ ($R^2 = 0.922$, $p < 0.0001$) values from the same samples to predict $\delta^{13}\text{C}$ of average primary production from which the EAA originated.

RESULTS

Bulk $\delta^{13}\text{C}$ values

Bulk $\delta^{13}\text{C}$ values in *Mytilus californianus* adductor muscle ranged between -18.0 and -13.0 ‰ at 28 stations spanning 11 degrees of latitude along the CA coast (Fig. 1). Several sites in central CA (SC and ML;

see Table 1 for site abbreviations) stood out as having the most enriched values (-13.4 ‰, -13.9 ‰, respectively) followed by SB (-14.4 ‰). SC and ML were also the 2 sites that had the greatest variability among individuals (± 0.9 ‰, $n = 10$; as opposed to average variability of ± 0.3 ‰ for all sites). In contrast, the 2 sites with the lowest $\delta^{13}\text{C}$ values (PCL and SCL; both -17.3 ‰) were widely geographically separated (PCL in northern CA, SCL in southern CA). Overall, bulk $\delta^{13}\text{C}$ values did not display any correlation with latitude ($R^2 = 0.022$; $p > 0.05$). When considered as a whole, the average of *Mytilus* $\delta^{13}\text{C}$ values over the entire CA coast dataset in fact fell into a very narrow range (-15.7 ± 0.9 ‰; Table 1, Fig. 2).

This suggests that on the whole, *Mytilus* data are recording a generally homogenous $\delta^{13}\text{C}$ value for CUE primary productivity, albeit marked by substantial inter-site variation (Fig. 1). A hierarchical cluster

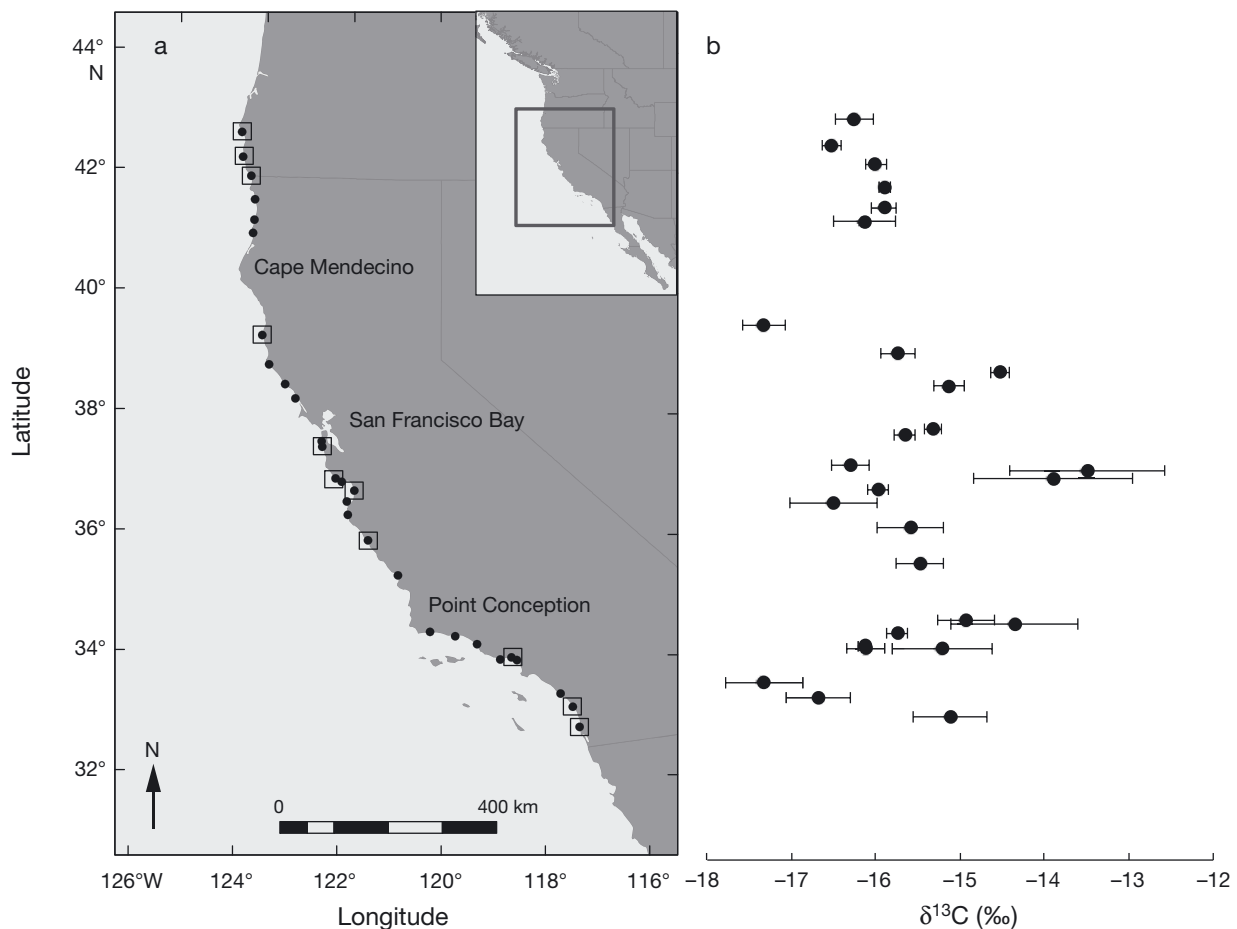


Fig. 1. *Mytilus californianus*. Site-specific bulk $\delta^{13}\text{C}$ values of mussels as a function of latitude in the context of a map of collection sites on the California coast, USA. (a) Filled circles indicate all sampling sites, and correspond directly to bulk analysis values in panel b; squares represent sites chosen for compound-specific isotope analysis. (b) Filled circles indicate average $\delta^{13}\text{C}$ for 5 individuals from each site; error bars indicate SD. While data indicate substantial (>4 ‰) inter-site variability, linear regression indicates no correlation of the $\delta^{13}\text{C}$ of suspended particle food sources with latitude ($R^2 = 0.02202$, $p > 0.05$)

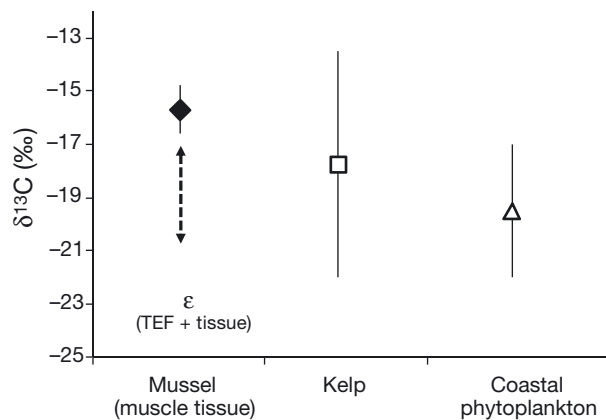


Fig. 2. *Mytilus californianus*. Mean bulk $\delta^{13}\text{C}$ for major coastal primary production sources vs. measured values for adductor muscle tissue. Endmember $\delta^{13}\text{C}$ values for coastal kelp (Clementz & Koch 2001, Foley & Koch 2010) and near-shore California, USA, upwelling zone phytoplankton production (data compiled by Clementz & Koch 2001) are both broad and overlapping. Degree of fractionation (ϵ ; indicated by dashed double-ended arrow) for the trophic enrichment factor (TEF) and specific tissue type are unknown

analysis also did not indicate that inter-site variability was strongly related to at least the basic habitat types we classified (e.g. rocky, sandy; see 'Materials and methods' and Table 1). However, we found strong location-specific variation in strength of local upwelling, and associated water chemistry, along the CA coast (Feely et al. 2008), as well as relative intensity of primary production (e.g. Walker & McCarthy 2012). Therefore, it seems most likely that $\delta^{13}\text{C}$ variation is related to variations in local oceanography, primary productivity, and/or the relative contribution of C sources at specific regions of the CA coastline.

AA $\delta^{13}\text{C}$ patterns in *Mytilus californianus*

Fig. 3 presents the first $\delta^{13}\text{C}_{\text{AA}}$ comprehensive data for a littoral mussel population, from a subset of sample sites ($n = 11$; Table 2) selected to encompass the range of both isotopic variability and geographic range. Normalized AA $\delta^{13}\text{C}$ values are arranged first

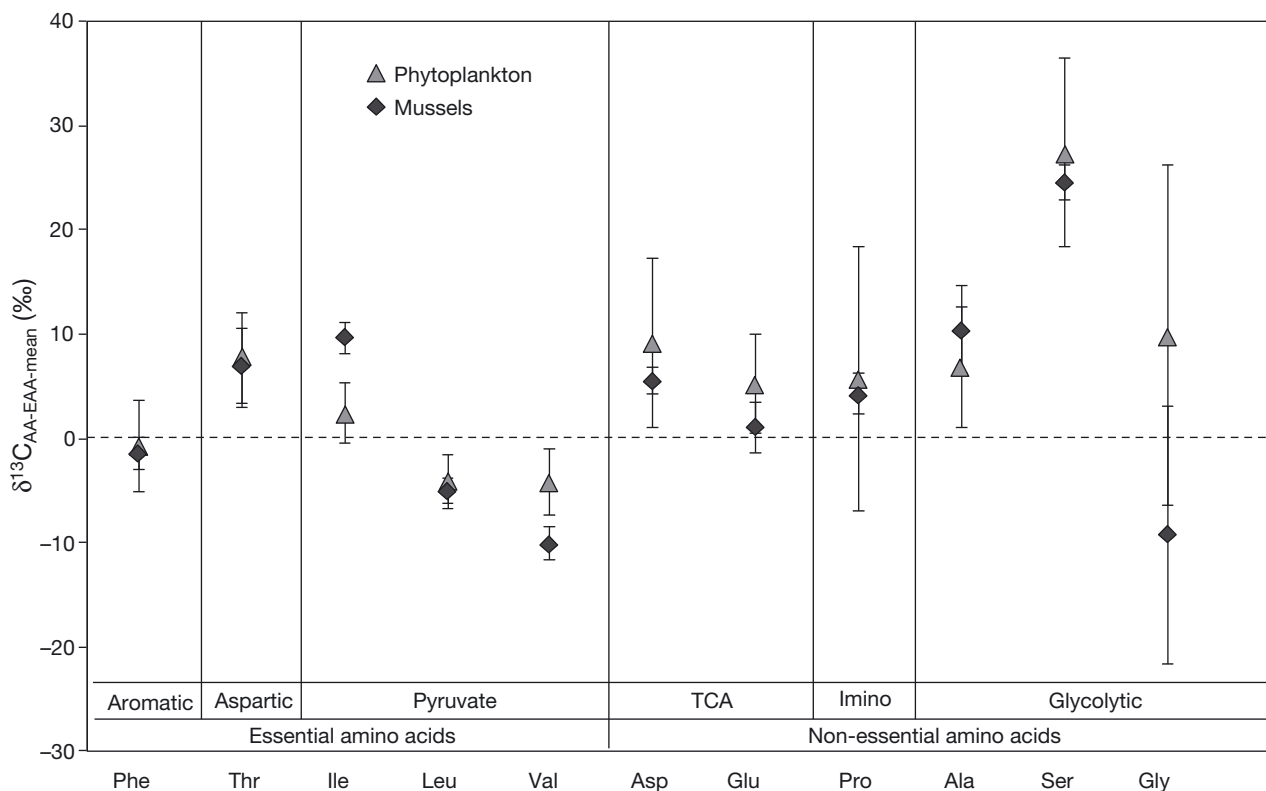


Fig. 3. *Mytilus californianus*. Patterns in $\delta^{13}\text{C}$ of amino acids ($\delta^{13}\text{C}_{\text{AA}}$) in mussels compared to those expected for marine phytoplankton. Mussel amino acid values (filled diamonds, $n = 11$) are normalized to average essential amino acid $\delta^{13}\text{C}$ ($\delta^{13}\text{C}_{\text{AA-EAA-mean}}$) to reveal $\delta^{13}\text{C}_{\text{AA}}$ biosynthetic pattern, independent of site-specific bulk $\delta^{13}\text{C}$ variation. Filled triangles ($n = 18$) represent similarly normalized $\delta^{13}\text{C}_{\text{AA}}$ pattern for eukaryotic marine phytoplankton (see 'Materials and methods' and Table S2 in the Supplement; www.int-res.com/articles/suppl/m504p059_supp.pdf). Amino acids are arranged first according to essential and non-essential groupings, and second by standard autotrophic biosynthetic families, with abbreviations as defined in text ('Compound-specific stable C isotope analysis'). TCA: tricarboxylic acid. Error bars indicate SD

Table 2. *Mytilus californianus*. Mean $\delta^{13}\text{C}$ values of bulk and compound-specific amino acids in mussels from selected sampling locations (site codes as in Table 1), grouped as essential and non-essential amino acids. For individual amino acid values, the mean \pm SE represents analytical variability ($n = 3$ injections) for a homogenized composite sample from all individuals sampled from each location; nd: no data

Site	Bulk	Essential amino acids					Non-essential amino acids					
		Phe	Thr	Ile	Leu	Val	Asp	Glu	Pro	Ala	Ser	Gly
HMPO	-16.3	-24.2 \pm 0.9	-21.2 \pm 0.1	-14.8 \pm 0.5	-28.8 \pm 0.5	-19.0 \pm 0.4	-17.6 \pm 0.2	-17.7 \pm 0.5	-17.6 \pm 0.7	-12.2 \pm 0.1	-0.3 \pm 0.2	-9.2 \pm 0.6
MCPR	-16.5	-25.2 \pm 0.4	-13.2 \pm 0.7	-12.4 \pm 0.5	-29.5 \pm 0.2	-18.4 \pm 0.5	-16.6 \pm 0.4	-21.4 \pm 0.2	-21.8 \pm 0.9	-18.5 \pm 0.7	0.3 \pm 0.6	-50.6 \pm 0.5
PSB	-16.0	-23.1 \pm 0.5	-12.7 \pm 0.4	-13.6 \pm 0.3	-30.1 \pm 1.3	-20.8 \pm 0.1	-17.8 \pm 0.2	-20.8 \pm 0.2	-20.7 \pm 0.2	-12.2 \pm 0.5	0.8 \pm 0.3	-27.7 \pm 0.5
PCL	-17.3	-27.0 \pm 0.5	-17.1 \pm 0.7	-16.2 \pm 0.7	-30.1 \pm 1.3	-19.8 \pm 0.2	-21.0 \pm 0.2	-25.8 \pm 0.2	-20.7 \pm 0.5	-14.9 \pm 0.0	2.3 \pm 0.2	-44.6 \pm 0.7
HMB	-15.7	-25.3 \pm 0.6	-23.5 \pm 0.3	-13.4 \pm 0.8	-28.4 \pm 0.2	-20.5 \pm 0.2	-18.0 \pm 0.1	-22.6 \pm 0.1	nd	-14.5 \pm 0.4	-2.7 \pm 0.2	-33.2 \pm 0.3
DAV	-16.3	-28.4 \pm 0.2	-13.2 \pm 0.1	-14.4 \pm 0.1	-28.7 \pm 0.1	-19.1 \pm 0.2	-19.3 \pm 0.1	-25.5 \pm 0.1	-18.8 \pm 0.1	nd	1.7 \pm 0.2	-31.2 \pm 0.8
ML	-13.9	-21.7 \pm 0.7	-20.1 \pm 0.5	-11.1 \pm 0.3	-28.7 \pm 0.9	-19.4 \pm 0.8	-15.4 \pm 0.3	-20.1 \pm 0.2	-18.5 \pm 0.4	-17.9 \pm 0.4	1.5 \pm 0.3	-36.0 \pm 0.5
MC	-15.6	-23.9 \pm 0.1	-10.5 \pm 0.2	-15.7 \pm 0.2	-27.3 \pm 0.3	-17.2 \pm 0.3	-17.6 \pm 0.1	-23.0 \pm 0.3	-17.6 \pm 0.1	-11.3 \pm 0.4	2.9 \pm 0.1	-21.9 \pm 0.9
TOP	-16.2	-25.8 \pm 1.0	-19.1 \pm 0.4	-14.6 \pm 0.4	-29.5 \pm 0.3	-17.7 \pm 0.3	-20.1 \pm 0.9	-22.3 \pm 0.5	nd	-17.7 \pm 0.1	-3.1 \pm 0.0	-46.4 \pm 0.4
OCE	-16.7	-26.4 \pm 1.2	-19.6 \pm 0.3	-15.0 \pm 0.1	-29.3 \pm 0.1	-22.2 \pm 0.0	-19.9 \pm 0.1	-25.1 \pm 0.3	-19.3 \pm 0.1	-11.7 \pm 0.0	0.2 \pm 0.3	-40.4 \pm 0.3
LAJ	-15.1	-25.5 \pm 0.8	-13.8 \pm 0.1	-14.1 \pm 0.1	-27.1 \pm 0.1	-18.3 \pm 0.1	-17.2 \pm 0.3	-25.1 \pm 0.2	-17.8 \pm 0.2	-9.3 \pm 0.3	5.5 \pm 0.2	-21.6 \pm 0.1

according to the EAA and NAA groupings, also indicating the major autotrophic biosynthetic families of AAs. The overall $\delta^{13}\text{C}_{\text{AA}}$ patterns were highly consistent for *Mytilus californianus* samples from all sites (Fig. 3). The average standard deviations of the NAA (excluding Gly) and EAA groups were $\pm 2.4\%$ and 2.1% , respectively. These patterns thus represent a common biosynthetic $\delta^{13}\text{C}_{\text{AA}}$ signature for *Mytilus* populations along the entire CA coast. Overall, the NAAs (Asp, Glu, Pro, Ala, Ser, and Gly) were significantly heavier (mean NAA group: -17.6%) than the EAA group (Phe, Thr, Ile, Leu, Val; mean EAA group: -20.7%). While GC-IRMS recovers most AAs, mole percent data show that the AAs measured by IRMS constituted 73% of the total AAs measured using a non-derivitized HPL approach (see Table S9 in the Supplement). Because isotope mass balances were close to 100%, this indicates that the AAs which could not be measured by GC-IRMS must have average isotopic values near the bulk isotope values.

Specific *Mytilus* $\delta^{13}\text{C}_{\text{AA}}$ patterns also generally corresponded closely to the individual biosynthetic families. For example, the anaplerotic AAs Glu and Asp, originating directly from the tricarboxylic acid (TCA) cycle, both had values that are within error of each other (t -test: $p > 0.05$), and these have in the past been used as proxies for TCA cycle C shuttle molecules (Scott et al. 2006). Leu and Val, both in the pyruvate group with closely related synthetic pathways (see Fig. S2 in the Supplement), also had very similar values. Ile, however, was enriched by more than 10% compared to Leu and Val, with values more similar to Thr. While Ile and Val share 4 enzymes in common (Buchanan et al. 2000), C of Ile is derived from Thr rather than directly from pyruvate (Fig. S2). Proline (Imino grouping) is synthesized from a glutamate precursor, and its value was also similar to Glu and Asp $\delta^{13}\text{C}$ values. Finally, the glycolytic AAs (Ala, Ser, and Gly) had the most variable values among all samples, which is most likely due to the fact that the C skeletons of these short-chain AAs are rapidly recycled in animal metabolism. In particular, Gly stood out among all other AAs as having the greatest variation in $\delta^{13}\text{C}$ values between sampling sites ($\text{SD} \pm 12\%$ versus 1–5% for all other AAs). In contrast to Gly, most other NAAs were not as strongly offset from expected algal source patterns.

Comparison to phytoplankton $\delta^{13}\text{C}$ -AA patterns

For EAA, we observed close similarity of normalized $\delta^{13}\text{C}_{\text{EAA}}$ patterns to those derived from disparate

phytoplankton sources (Fig. 3). Data for marine phytoplankton $\delta^{13}\text{C}_{\text{AA}}$ patterns was compiled from 2 recent studies (Lehman 2009, Larsen et al. 2013) for a range of cosmopolitan eukaryotic and prokaryotic photosynthetic species (see Table S2 in the Supplement). The $\delta^{13}\text{C}_{\text{EAA}}$ patterns matched very well: most values were not statistically different for both *Mytilus* and the average phytoplankton pattern (Fig. 3); *t*-tests indicated no significant differences for Phe, Thr, and Leu ($p > 0.05$); however, Ile and Val both had offsets that were significantly different (both $p < 0.0001$).

For phytoplankton, the collective variability versus the algal $\delta^{13}\text{C}_{\text{AA}}$ pattern was much larger for the NAA group (Fig. 3, NAA and EAA mean SD: ± 9.6 and 3.4‰ , respectively). Due possibly to this increased variability, offsets from the algal pattern for most of the NAAs were not significant (Asp, Pro, Ala, and Ser, $p > 0.05$); however, there were large and significant differences for Glu ($p < 0.05$) and Gly ($p < 0.001$).

LDA model results

Our LDA model based on the training set from Larsen et al. (2013) predicted that marine microalgae were the most likely protein source (probability $\geq 92\%$) for 10 out of 11 mussel samples (Fig. 4, Table S1 in the Supplement); the remaining sample had Phaeophyceae as the most likely protein source (probability = 74%). None of 13 mussel samples had bacterial $\delta^{13}\text{C}_{\text{EAA}}$ patterns, indicating that protein contributions from microbially re-worked detritus were relatively small compared to the 2 algal sources. We also included 2 mussel samples from Larsen et al. (2013) in the LDA model to validate the inter-laboratory calibration of $\delta^{13}\text{C}_{\text{EAA}}$ values, and both samples had $\delta^{13}\text{C}_{\text{EAA}}$ patterns resembling microalgae (probability $\geq 98\%$). Taken together with the relatively low standard deviation values for the inter-laboratory calibration (1.2‰ on average; Table S5 in the Supplement), this demonstrates that our results are not tied to any specific $\delta^{13}\text{C}$ analytical protocol. The inter-laboratory calibration approach has also been tested successfully on samples from sea turtles (Arthur et al. in press).

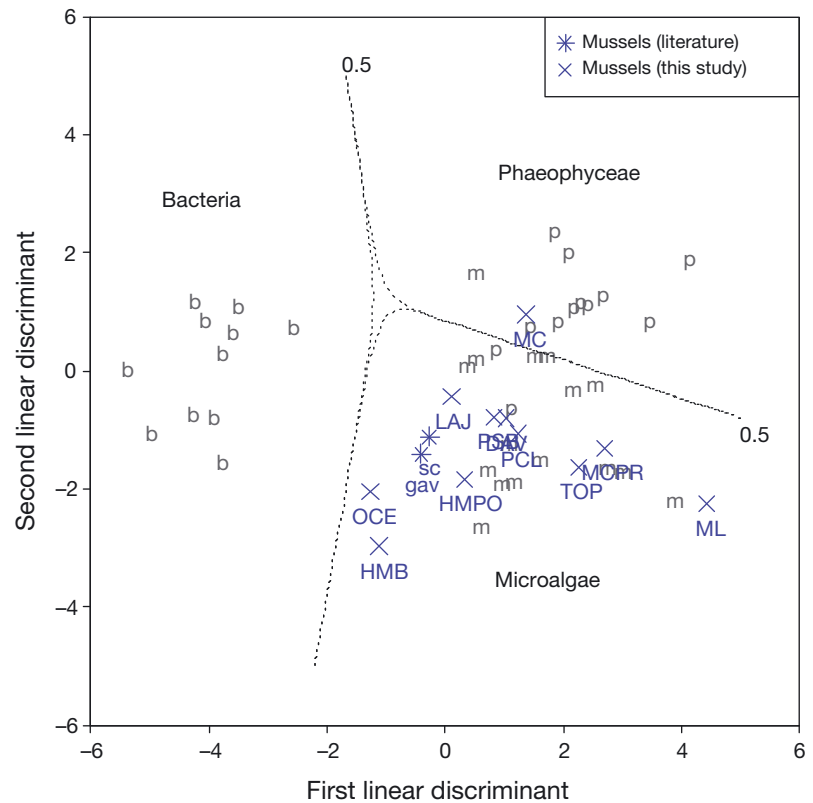


Fig. 4. Linear discriminant analysis (LDA) plot based on $\delta^{13}\text{C}$ values of 5 essential amino acids (EAAs: Ile, Leu, Phe, Thr, Val) from 3 categorical variables, viz. marine microalgae (m, $n = 16$), bacteria (b, $n = 12$), and Phaeophyceae (p, $n = 12$; including *Macrocystis* kelp), from Larsen et al. (2013) to predict the biosynthetic origins of EAAs among mussels *Mytilus californianus*. Mussel $\delta^{13}\text{C}_{\text{EAA}}$ values originate from this study ($n = 10$, labels in capital letters) and Larsen et al. (2013) ($n = 2$, labels in lowercase letters). All mussels classified with an average of 96% probability as microalgae except for MC, which classified with 75% as Phaeophyceae. Sample site abbreviations are as defined in Table 1 (mussels). See Table S1 in the Supplement for LDA output

DISCUSSION

Bulk $\delta^{13}\text{C}$ values: implications for major *Mytilus* C sources

Possible main sources to the CUE-suspended particulate organic matter pool include local or laterally advected phytoplankton and perhaps terrestrial material or partially degraded marine detritus (Fig. 2). The uniformly heavy mussel $\delta^{13}\text{C}$ values (Fig. 1) would seem to preclude the possibility of significant terrestrial detrital contribution, since $\delta^{13}\text{C}$ signatures of terrestrial C (C3 sources) are typically much lighter (-26 and -28‰ ; e.g. Smith & Epstein 1971). This is perhaps not surprising, given the relative scarcity of riverine input into most regions sampled, as well as the relatively degraded (i.e. low nutritive value) nature of detrital humic materials delivered

from soils (Simenstad & Wissmar 1985, Howarth et al. 1991, Rau et al. 2001).

In contrast, giant kelp *Macrocystis pyrifera* is the dominant primary producer in littoral ecosystems along the CA coast (Dayton 1985, Duggins et al. 1989, Graham et al. 2007) and is considered a food source for many suspension feeders (Miller & Page 2012). In many locations, kelp also has very high $\delta^{13}\text{C}$ values, directly within the range of our measured mussel values (e.g. Clementz & Koch 2001, Foley & Koch 2010). Further, while offshore micro-agal production typically has low $\delta^{13}\text{C}$ values (Rau et al. 1982, Goericke & Fry 1994), the $\delta^{13}\text{C}$ values of marine phytoplankton in highly productive upwelling regions can be substantially isotopically heavier but can in fact also vary quite widely (e.g. -17.0 to -22.0‰ ; Rau et al. 2001, Walker & McCarthy 2012).

Finally, trophic and tissue-specific isotope offsets further complicate direct bulk $\delta^{13}\text{C}$ interpretation. Measured $\delta^{13}\text{C}$ values would first be expected to have a TEF associated with a primary consumer; such fractionations are often assumed to be small ($\sim 0.7\text{‰}$; DeNiro & Epstein 1978), but more recent work has increasingly demonstrated that TEF can in fact vary widely (between ~ 0.6 and 3.0‰ ; Gannes et al. 1997, Vander Zanden & Rasmussen 2001, McCutchan et al. 2003, Olive et al. 2003, McMahan et al. 2010). In addition, a specific tissue of any organism has the potential for a tissue-specific fractionation, based on either isotopic routing or well-known biochemical class differences (Jim et al. 2006). The adductor muscle tissue is composed almost entirely of protein, so would generally be expected to have heavier $\delta^{13}\text{C}$ values versus total biomass (Vander Zanden & Rasmussen 2001); however, without organism-specific data, the exact magnitude of such offsets is impossible to predict.

***Mytilus californianus* EAA versus NAA $\delta^{13}\text{C}$ patterns**

The comparison of *Mytilus* $\delta^{13}\text{C}_{\text{AA}}$ patterns to those in phytoplankton (Fig. 3) directly addresses the hypothesis that EAA in filter-feeding consumers may be useful both as new, more specific, source tracers, and also as proxies for integrated $\delta^{13}\text{C}$ values of primary production. Our results concerning the behavior of EAAs are strongly consistent with direct, unaltered linkage to primary production sources. Overall, this correspondence supports our basic hypothesis that EAAs in these filter feeders directly record the isotopic values of primary production from local pri-

mary production. $\delta^{15}\text{N}_{\text{AA}}$ data also strongly support that marine algae have essentially universal CSI-AA signatures (e.g. Chikaraishi et al. 2009, McCarthy et al. 2013), which indicates that $\delta^{13}\text{C}_{\text{AA}}$ can also be used as a baseline pattern to both trace sources and understand heterotrophic transformation (Larsen et al. 2009, 2012).

Results for the NAA groupings are less easy to interpret but are also consistent with previous controlled feeding studies, indicating that NAA fractionation can be variable, based on both diet composition and individual metabolism (e.g. McMahan et al. 2010). Large trophic fractionations have been observed only in selected $\delta^{13}\text{C}_{\text{NAA}}$, coupled with little to no fractionation in $\delta^{13}\text{C}_{\text{EAA}}$ (e.g. Howland et al. 2003, Jim et al. 2006, McMahan et al. 2010). The most dramatic NAA $\delta^{13}\text{C}$ offset in our data set was the substantial depletion of Gly in *Mytilus* compared to algae; this might at first seem unusual, based on typical expectations for isotope enrichment with trophic fractionation. However, while Gly has been reported with enriched AA values in some feeding studies, as noted above this AA also typically has the highest variability (Howland et al. 2003, Jim et al. 2006, McMahan et al. 2010). In particular, light Gly $\delta^{13}\text{C}$ values versus diet have also been documented in previous controlled studies (McMahan et al. 2010). This has been interpreted to be due to catabolized dietary lipids being used as a significant energy source (Post et al. 2007) and thus providing a strongly ^{13}C -light C pool for Gly synthesis (e.g. DeNiro & Epstein 1978, McMahan et al. 2010). We find the idea of Gly as a metabolic marker of food quality intriguing, but we feel it is too speculative for application to field-derived data such as ours, where ^{13}C -Gly values may also be influenced by metabolic processes in both mussels and their food sources. Plants use several pathways to synthesize Gly (see Fig. S2 in the Supplement), depending on the degree of photorespiration. Animals can readily synthesize Gly, but rates are likely controlled by protein synthetic needs (Jim et al. 2006). A carefully designed study with defined food sources and treatments could help to investigate this promising idea. For the other NAAs, while there is clear evidence for resynthesis shown in the significant offset between phytoplankton versus mussel Glu and Gly $\delta^{13}\text{C}$ values (Fig. 3), our results generally suggest that direct incorporation from diet seems to dominate for most other NAAs in *Mytilus*. This would also be consistent with a relatively protein-rich diet (e.g. plankton), as direct incorporation is strongly energetically favored versus de novo synthesis whenever sufficient AAs are available (Jim et al. 2006).

CSI-AA source fingerprinting

The strong correspondence of *Mytilus* $\delta^{13}\text{C}_{\text{NAA}}$ patterns to marine phytoplankton supports the use of isotope fingerprinting to directly trace phylogeny of main C sources. As noted above, mussel bulk $\delta^{13}\text{C}$ values are ambiguous: most fall within $\delta^{13}\text{C}$ ranges typical for *Macrocystis* (Foley & Koch 2010); however, they could also be consistent with ^{13}C -enriched coastal algal production (Fry & Wainright 1991, Rau et al. 1992, 2001, Hemminga & Mateo 1996). Further, because bacterial degradation typically does not greatly affect bulk $\delta^{13}\text{C}$ values (Fogel et al. 1989, Benner et al. 1992, Fogel & Tuross 1999, McCarthy et al. 2004), bulk isotope values cannot rule out suspended detrital sources. The LDA results strongly indicate that despite substantial variation in bulk $\delta^{13}\text{C}$ values (Fig. 2), mussels at almost all locations examined along the CA coast feed mainly on phytoplankton, with only minimal food web connection to kelp primary production and/or re-worked detritus. To our knowledge, these results represent the first comprehensive application of diagnostic $\delta^{13}\text{C}_{\text{EAA}}$ patterns to a geographically widely distributed population in any species.

A conclusion of a dominant microalgal food source for mussels is consistent with work on mussel ecology (Widdows et al. 1979, Dame & Prins 1997, Bracken et al. 2012), as well as reduction of phytoplankton biomass over intertidal mussel beds (Asmus & Asmus 1991). However, the real importance of this result is the clear demonstration that $\delta^{13}\text{C}_{\text{EAA}}$ values can address fundamental ambiguity in bulk $\delta^{13}\text{C}$ values. The ability of $\delta^{13}\text{C}_{\text{EAA}}$ patterns to clearly indicate a dominant food source (which is also ecologically consistent), strongly underscores the potential of CSI-AA to detangle food web C sources in systems where multiple sources of primary production are plausible. This is also consistent with previous $\delta^{13}\text{C}_{\text{EAA}}$ fingerprinting results in other complex systems such as mangroves (Larsen et al. 2012), pelagic, and freshwater ecosystems (Larsen et al. 2013). However, we also note that the LDA is not suited for quantitative accounting of relative contributions of mixed sources. For quantitative applications from such data, Bayesian isotopic mixing models are required. Larsen et al. (2013) recently demonstrated a CSI-AA Bayesian isotopic mixing approach for *Mytilus californianus*, suggesting that all specimens obtained about two-thirds of their EAAs from microalgae, about a quarter from kelp, and the remaining (small) fraction from bacteria. Since most of our mussel samples had $\delta^{13}\text{C}_{\text{EAA}}$ patterns that resemble those reported

by Larsen et al. (2013) (Fig. 4), we conclude that while microalgae are the dominant source for *M. californianus*, it is also possible that macroalgae and microbial derived sources could make smaller contributions.

Using $\delta^{13}\text{C}_{\text{EAA}}$ values to estimate integrated $\delta^{13}\text{C}$ of primary production

The ability of isotope fingerprints to indicate major sources, coupled with unaltered $\delta^{13}\text{C}_{\text{EAA}}$ values through food webs, suggests that $\delta^{13}\text{C}_{\text{EAA}}$ in littoral mussels constitutes a powerful new approach to reconstruct integrated isotopic patterns of coastal primary production. The feasibility of this, however, depends on several basic assumptions. First, EAAs are assumed to be incorporated from reasonably well-defined sources, with little microbial alteration. As noted above, together the mussel $\delta^{13}\text{C}_{\text{EAA}}$ fingerprinting data (Figs. 4 & 5), and the close match for $\delta^{13}\text{C}_{\text{EAA}}$ patterns with marine phytoplankton (Fig. 3), strongly support a direct phytoplankton source for these molecules. The $\delta^{13}\text{C}_{\text{EAA}}$ in mussels therefore likely represents average EAA from littoral/coastal phytoplankton sources, integrated over turnover times for the tissue type sampled (adductor muscle). Finally, in order to directly 'back calculate' a $\delta^{13}\text{C}$ value for original primary production from measured $\delta^{13}\text{C}$ values, there must be a consistent offset between $\delta^{13}\text{C}_{\text{EAA}}$ and bulk $\delta^{13}\text{C}$ in sources, so that a

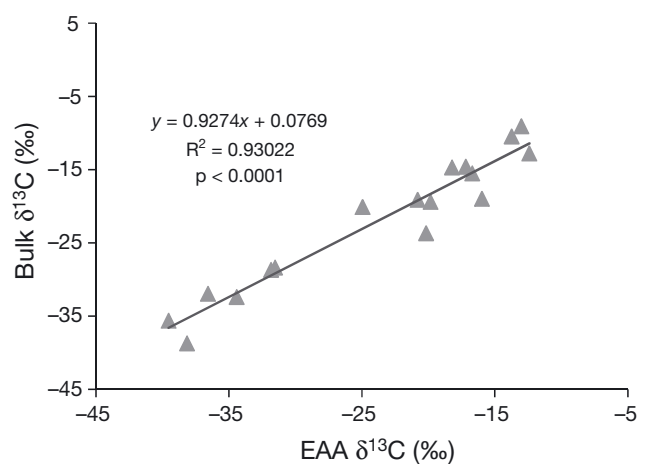


Fig. 5. Relationship between $\delta^{13}\text{C}$ values of bulk vs. average essential amino acids (EAAs: Phe, Thr, Leu, Ile, Val) in photoautotrophs ($n = 19$). The strong correlation indicates a consistent offset between bulk and EAAs $\delta^{13}\text{C}$ values. The equation of this relationship can potentially be used to predict source micro-algal production bulk values from a consumer's average $\delta^{13}\text{C}_{\text{EAA}}$

correction can be made. The strong linear correlation that we found between bulk $\delta^{13}\text{C}$ and $\delta^{13}\text{C}_{\text{EAA}}$ phytoplankton across diverse cultured and environmental algal samples (Fig. 5) strongly supports this last condition.

We tested this overall idea by using the equation of the line for the bulk versus $\delta^{13}\text{C}_{\text{EAA}}$ relationship in algae to estimate bulk $\delta^{13}\text{C}$ values for coastal phytoplankton primary production at the sites selected for CSI-AA between southern Oregon ($42^\circ 43' \text{N}$) and La Jolla, CA ($32^\circ 51' \text{N}$). The resulting values ranged from -20.2 to -23.5‰ (Table 2, Fig. 6), with an overall average of $-21.9 \pm 1.2\text{‰}$. A substantial enrichment of $\delta^{13}\text{C}$ values in bulk adductor muscle relative to the predicted average phytoplankton food $\delta^{13}\text{C}$ values ($\sim 4\text{‰}$; Fig. 6) is consistent with several expectations. First, protein has elevated $\delta^{13}\text{C}$ values compared to other compound classes (DeNiro & Epstein 1978), so the bulk adductor muscle tissue would therefore be expected to have enriched bulk $\delta^{13}\text{C}$ values versus the overall mussel biomass (not measured). Second, trophic transfer will cause further (but as noted above, poorly defined) ^{13}C enrichment in the mussel compared to its algal food source. Finally, the observation that the exact $\delta^{13}\text{C}$ offset between adductor muscle tissue and estimated phytoplankton bulk $\delta^{13}\text{C}$ values (directly linked to $\delta^{13}\text{C}_{\text{EAA}}$) is not exactly constant is also expected ($R^2 = 0.1904$), since variable degrees of resynthesis in the NAA pool with trophic transfer for different location/populations should slightly decouple these values.

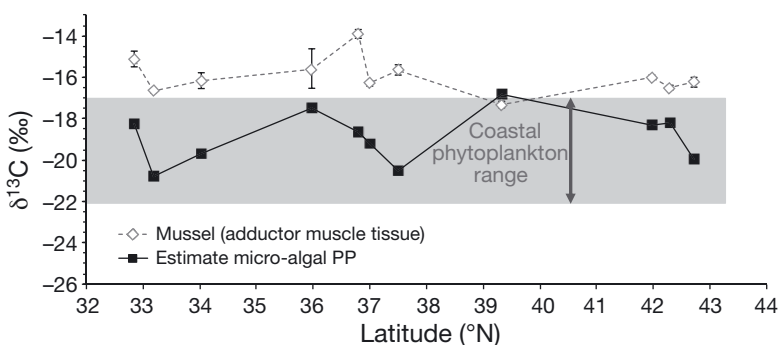


Fig. 6. Integrated yearly average $\delta^{13}\text{C}$ value of California, USA, coastal primary production (PP) estimated from essential amino acids (EAA) (filled squares; average -20.9‰), vs. measured $\delta^{13}\text{C}$ values for bulk muscle tissue samples (open diamonds; average -16.0‰). The shaded gray box is the expected average range of $\delta^{13}\text{C}$ values of coastal phytoplankton \pm SD (compiled by Clementz & Koch 2001). The enriched $\delta^{13}\text{C}$ values in mussels represent the combined effects of trophic and tissue-specific fractionations, demonstrating the potential for EAA $\delta^{13}\text{C}$ values to directly indicate original PP isotopic values. A moving average line shows the overall pattern with latitude on the California coast; see the 'Discussion' for calibration calculations of estimated PP

Overall, our 'reconstructed' values for primary production fall approximately within the range expected for inshore phytoplankton $\delta^{13}\text{C}$ values in the CUE, based on past work (e.g. Clementz & Koch 2001; see Fig. 6), strongly supporting the validity of this new approach. Further, while the relative changes in projected phytoplankton $\delta^{13}\text{C}$ track those in bulk $\delta^{13}\text{C}$ values, the amplitude of variation is also substantially greater for reconstructed values (Fig. 6). Since $\delta^{13}\text{C}_{\text{EAA}}$ values are unaffected by variable AA resynthesis versus incorporation or routing, we hypothesize that the $\delta^{13}\text{C}$ record based on $\delta^{13}\text{C}_{\text{EAA}}$ more accurately reflects actual spatial variation in phytoplankton $\delta^{13}\text{C}$ than traditional bulk measurements. If our assumptions about integration times for this mussel size class/tissue type are accurate, then our CSI-AA based record implies substantial variation in average phytoplankton production $\delta^{13}\text{C}$ for specific zones along the CA coast. This would be consistent with zonal variations in coastal upwelling (Hickey 1998, Pennington & Chavez 2000, Checkley & Barth 2009) and surface water pH (Feely et al. 2008), as well as prior work documenting major region-specific $\delta^{13}\text{C}$ variations noted above (Walker & McCarthy 2012). If the variations we document are confirmed by future sampling, $\delta^{13}\text{C}_{\text{EAA}}$ in coastal mussels represent a new, highly detailed, approach to mapping both geographic and possibly inter-annual variation in isotopic signatures of coastal phytoplankton production.

SUMMARY

This study has presented the largest $\delta^{13}\text{C}_{\text{AA}}$ dataset for a common filter-feeding mollusk, examining both details of the $\delta^{13}\text{C}_{\text{AA}}$ patterns and also specific offsets between EAA $\delta^{13}\text{C}$ and NAA $\delta^{13}\text{C}$ values across a wide geographic range on the CA coastline. Our ultimate goal has been to assess whether $\delta^{13}\text{C}$ patterns of the essential AA group in littoral mussels *Mytilus californianus* can constitute a new approach to determine integrated stable isotope values for coastal primary production.

Biosynthetic $\delta^{13}\text{C}_{\text{AA}}$ patterns (with the exception of Gly) were essentially identical in all mussels sampled, with variation in specific AA values determined by bulk $\delta^{13}\text{C}$ offsets between sampling sites.

Overall, the specific comparison to $\delta^{13}\text{C}_{\text{EAA}}$ patterns from marine algae strongly supports the hypothesis that EAAs are incorporated directly into mussel tissue, with little to no isotopic alteration. The most widespread application to date of multivariate $\delta^{13}\text{C}_{\text{EAA}}$ source fingerprinting further indicated that the dominant EAA source for all mussels was phytoplankton, with no evidence for substantial EAA contributions from either *Macrocystis* (or other local *Phaeocystis* algae), or potentially microbially altered detrital sources. Together, these results imply that for EAAs in mussels along the CA coast, measured $\delta^{13}\text{C}$ values dominantly reflect an integrated signature for coastal phytoplankton production $\delta^{13}\text{C}$ values at each sampling location. We therefore used the strong linear relationship observed between $\delta^{13}\text{C}_{\text{EAA}}$ and bulk $\delta^{13}\text{C}$ values in currently available data for marine phytoplankton to determine the correlation between bulk plankton and average EAA $\delta^{13}\text{C}$ values. Using this relationship, we show that $\delta^{13}\text{C}$ values for source primary production may be 'reconstructed' from measured $\delta^{13}\text{C}_{\text{EAA}}$. Our resulting predictions fall within reasonable ranges for CA coastal phytoplankton $\delta^{13}\text{C}$ values (Fig. 6).

Taken together, these observations may have widespread implications for several key aspects of ecological studies. First, we have shown that in a system in which bulk $\delta^{13}\text{C}$ values are inherently ambiguous with respect to multiple possible C sources, $\delta^{13}\text{C}_{\text{EAA}}$ analysis can bypass both tissue-specific and trophic-related fractions, to identify major primary production C sources, suggesting wide applicability of $\delta^{13}\text{C}_{\text{EAA}}$ fingerprinting in other marine consumers, where a complex mix of C sources are likely. Our results also suggest a new approach for the construction of more accurate and highly detailed ecosystem-wide $\delta^{13}\text{C}$ isoscapes, with new potential to overcome many of the inherent issues associated with bulk isotope analysis in consumers (Graham et al. 2010). Isoscapes inherently link the effects of broad geochemical processes with marine ecological dynamics, so it is critical to be able to decouple the effects of heterotrophic fractionation from the signatures of baseline C source. We suggest that compound-specific measurement of $\delta^{13}\text{C}_{\text{EAA}}$ will allow direct estimation of $\delta^{13}\text{C}$ values from primary production. Use of a specific tissue in filter feeders (like mussels) further allows determination of integrated baseline values which both average out high-frequency variability and can be chosen based on a turnover rate integrating yearly, seasonal, or possibly or even higher-resolution variability (Gorokhova & Hansson 1999). Moreover, isoscapes constructed using CSI-AA from mussels are not strictly limited to

coastlines. Mussels frequently attach to the base of fixed moorings located offshore (e.g. www.mbari.org/oasis/index.html), suggesting the potential to use this approach for long-term average isoscapes in conjunction with detailed oceanographic data at well-studied locations. Isotope fingerprints have also been used to distinguish between pelagic and estuarine sources among consumers migrating between both habitats (Arthur et al. in press). We suggest that to fully apply this approach, future work needs to focus on a more precise determination of the linear $\delta^{13}\text{C}$ bulk to EAA relationship for representative groups of marine primary producers. Finally, these results are also the first widespread demonstration of the recently described $\delta^{13}\text{C}_{\text{EAA}}$ source fingerprinting approach (Larsen et al. 2009, 2012, 2013).

Acknowledgements. We thank N. Quintana-Krupinsky, F. Batista, E. Gier, and D. Andreasen for helping to collect, prepare, and/or process samples; J. Felis for support on map construction; and T. Broek for additional analysis. Funding was provided by the National Science Foundation (NSF OCE-1131816), the UCSC Committee on Research (COR), as well as grants from The Friends of Long Marine Lab and the Myers Family Oceanographic Trust. This work was conducted under a permit from the California Department of Fish and Wildlife.

LITERATURE CITED

- Altabet MA (1996) Nitrogen and carbon isotopic tracers of the source and transformation of particles in the deep-sea. In: Ittekkot V, Schafer P, Honjo S, Depetris PJ (eds) Particle flux in the ocean. Wiley, London, p 155–184
- Arthur KE, Kelez S, Larsen T, Choy CA, Popp BN (2014) Tracing the biosynthetic source of essential amino acids in marine turtles using $\delta^{13}\text{C}$ fingerprints. Ecology (in press), doi: 10.1890/13-0263.1
- Asmus R, Asmus H (1991) Mussel beds: limiting or promoting phytoplankton? J Exp Mar Biol Ecol 148:215–232
- Aurioles D, Koch PL, Le Boeuf BJ (2006) Differences in foraging location of Mexican and California elephant seals: evidence from stable isotopes in pups. Mar Mamm Sci 22:326–338
- Barnes C, Jennings S, Barry JT (2009) Environmental correlates of large-scale spatial variation in the $\delta^{13}\text{C}$ of marine animals. Estuar Coast Shelf Sci 81:368–374
- Benner R, Pakulski JD, McCarthy M, Hedges JI, Hatcher PG (1992) Bulk chemical characteristics of dissolved organic matter in the ocean. Science 255:1561–1564
- Bracken MES, Menge BA, Foley MM, Sorte CJB, Lubchenco J, Schiel DR (2012) Mussel selectivity for high-quality food drives carbon inputs into open-coast intertidal ecosystems. Mar Ecol Prog Ser 459:53–62
- Broek TA, Walker BD, Andreasen DH, McCarthy MD (2013) High-precision measurement of phenylalanine $\delta^{15}\text{N}$ values for environmental samples: a new approach coupling high-pressure liquid chromatography purification and elemental analyzer isotope ratio mass spectrometry. Rapid Commun Mass Spectrom 27:2327–2337

- Buchanan BB, Gruissem W, Jones RL (2000) Biochemistry and molecular biology of plants. American Society of Plant Physiologists, Rockville, MD
- Burton RK, Snodgrass JJ, Gifford-Gonzalez D, Guilderson T, Brown T, Koch PL (2001) Holocene changes in the ecology of northern fur seals: insights from stable isotopes and archaeofauna. *Oecologia* 128:107–115
- Checkley DM Jr, Barth JA (2009) Patterns and processes in the California Current System. *Prog Oceanogr* 83:49–64
- Chikaraishi Y, Ogawa NO, Kashiyama Y, Takano Y and others (2009) Determination of aquatic food-web structure based on compound-specific nitrogen isotopic composition of amino acids. *Limnol Oceanogr Methods* 7: 740–750
- Clementz MT, Koch PL (2001) Differentiating aquatic mammal habitat and foraging ecology with stable isotopes in tooth enamel. *Oecologia* 129:461–472
- Cloern JE, Canuel EA, Harris D (2002) Stable carbon and nitrogen isotope composition of aquatic and terrestrial plants of the San Francisco Bay estuarine system. *Limnol Oceanogr* 47:713–729
- Dame R, Prins T (1997) Bivalve carrying capacity in coastal ecosystems. *Aquat Ecol* 31:409–421
- Dayton PK (1985) Ecology of kelp communities. *Annu Rev Ecol Syst* 16:215–245
- DeNiro MJ, Epstein S (1978) Influence of diet on the distribution of carbon isotopes in animals. *Geochim Cosmochim Acta* 42:495–506
- Dobush GR, Ankney CD, Kremenz DG (1985) The effect of apparatus, extraction time, and solvent type on lipid extractions of snow geese. *Can J Zool* 63:1917–1920
- Duggins DO, Simenstad CA, Estes JA (1989) Magnification of secondary production by kelp detritus in coastal marine ecosystems. *Science* 245:170–173
- Feely RA, Sabine CL, Hernandez-Ayon JM, Ianson D, Hales B (2008) Evidence for upwelling of corrosive 'acidified' water onto the continental shelf. *Science* 320:1490–1492
- Fogel ML, Tuross N (1999) Transformation of plant biochemicals to geological macromolecules during early diagenesis. *Oecologia* 120:336–346
- Fogel ML, Tuross N (2003) Extending the limits of paleo-dietary studies of humans with compound specific carbon isotope analysis of amino acids. *J Archaeol Sci* 30:535–545
- Fogel ML, Sprague EK, Gize AP, Frey RW (1989) Diagenesis of organic matter in salt marshes. *Estuar Coast Shelf Sci* 28:211–230
- Foley MM, Koch PL (2010) Correlation between allochthonous subsidy input and isotopic variability in the giant kelp *Macrocystis pyrifera* in central California, USA. *Mar Ecol Prog Ser* 409:41–50
- Fry B, Wainright SC (1991) Diatom sources of ^{13}C -rich carbon in marine food webs. *Mar Ecol Prog Ser* 76:149–157
- Fry B, Sherr EB (1984) $\delta^{13}\text{C}$ measurements as indicators of carbon flow in marine and freshwater ecosystems. *Contrib Mar Sci* 27:13–47
- Gannes LZ, O'Brien DM, Martínez del Rio C (1997) Stable isotopes in animal ecology: assumptions, caveats, and a call for more laboratory experiments. *Ecology* 78:1271–1276
- Goericke R, Fry B (1994) Variations of marine plankton $\delta^{13}\text{C}$ with latitude, temperature, and dissolved CO_2 in the world ocean. *Global Biogeochem Cycles* 8:85–90
- Gorokhova E, Hansson S (1999) An experimental study on variations in stable carbon and nitrogen isotope fractionation during growth of *Mysis mixta* and *Neomysis integer*. *Can J Fish Aquat Sci* 56:2203–2210
- Graham MH, Vasquez JA, Buschmann AH (2007) Global ecology of the giant kelp *Macrocystis*: from ecotypes to ecosystems. *Oceanogr Mar Biol Annu Rev* 45:39–88
- Graham BS, Koch PL, Newsome SD, McMahon KW, Aurioules D (2010) Using isoscapes to trace the movements and foraging behavior of top predators in oceanic ecosystems. In: West J, Bowen GJ, Dawson TE, Tu KP (eds) *Isoscapes: understanding movement, pattern, and process on Earth through isotope mapping*. Springer-Verlag, New York, NY, p 299–318
- Hansson S, Hobbie JE, Elmgren R, Larsson U, Fry B, Johansson S (1997) The stable nitrogen isotope ratio as a marker of food web interactions and fish migration. *Ecology* 78: 2249–2257
- Hemminga MA, Mateo MA (1996) Stable carbon isotopes in seagrasses: variability in ratios and use in ecological studies. *Mar Ecol Prog Ser* 140:285–298
- Hickey BM (1998) Coastal oceanography of western North America from the tip of Baja California to Vancouver Island. In: Robinson AR, Brink KH (eds) *The sea, the global coastal ocean*, Vol 11. John Wiley & Sons, New York, NY, p 345–393
- Hobson KA, Barnett-Johnson R, Cerling T (2010) Using isoscapes to track animal migration. In: West J, Bowen GJ, Dawson TE, Tu KP (eds) *Isoscapes: understanding movement, pattern, and process on Earth through isotope mapping*. Springer-Verlag, New York, NY, p 273–298
- Howarth RW, Fruci JR, Sherman D (1991) Inputs of sediment and carbon to an estuarine ecosystem: influence of land use. *Ecol Appl* 1:27–39
- Howland MR, Corr LT, Young SMM, Jones V and others (2003) Expression of the dietary isotope signal in the compound-specific $\delta^{13}\text{C}$ values of pig bone lipids and amino acids. *Int J Osteoarchaeol* 13:54–65
- Jim S, Jones V, Ambrose SH, Evershed RP (2006) Quantifying dietary macronutrient sources of carbon for bone collagen biosynthesis using natural abundance stable carbon isotope analysis. *Br J Nutr* 95:1055
- Kaehler S, Pakhomov EA, Kalin RM, Davis S (2006) Trophic importance of kelp-derived suspended particulate matter in a through-flow sub-Antarctic system. *Mar Ecol Prog Ser* 316:17–22
- Larsen T, Taylor DL, Leigh MB, O'Brien DM (2009) Stable isotope fingerprinting: a novel method for identifying plant, fungal, or bacterial origins of amino acids. *Ecology* 90:3526–3535
- Larsen T, Wooller MJ, Fogel ML, O'Brien DM (2012) Can amino acid carbon isotope ratios distinguish primary producers in a mangrove ecosystem? *Rapid Commun Mass Spectrom* 26:1541–1548
- Larsen T, Ventura M, Andersen N, O'Brien DM, Piatkowski U, Carthy MD (2013) Tracing carbon sources through aquatic and terrestrial food webs using amino acid stable isotope fingerprinting. *PLoS ONE* 8:e73441
- Lehman J (2009) Compound-specific amino acid isotopes as tracers of algal central metabolism: developing new tools for tracing prokaryotic vs. eukaryotic primary production and organic nitrogen in the ocean. MSc thesis, University of California, Santa Cruz, CA
- McCarthy MD, Benner R, Lee C, Hedges JI, Fogel ML (2004) Amino acid carbon isotopic fractionation patterns in oceanic dissolved organic matter: an unaltered photoautotrophic source for dissolved organic nitrogen in the ocean? *Mar Chem* 92:123–134

- McCarthy MD, Lehman J, Kudela R (2013) Compound-specific amino acid $\delta^{15}\text{N}$ patterns in marine algae: tracer potential for cyanobacterial vs. eukaryotic organic nitrogen sources in the ocean. *Geochim Cosmochim Acta* 103: 104–120
- McCutchan JH Jr, Lewis WM Jr, Kendall C, McGrath CC (2003) Variation in trophic shift for stable isotope ratios of carbon, nitrogen, and sulfur. *Oikos* 102:378–390
- McMahon KW, Fogel ML, Elsdon TS, Thorrold SR (2010) Carbon isotope fractionation of amino acids in fish muscle reflects biosynthesis and isotopic routing from dietary protein. *J Anim Ecol* 79:1132–1141
- McMahon KW, Berumen ML, Mateo I, Elsdon TS, Thorrold SR (2011) Carbon isotopes in otolith amino acids identify residency of juvenile snapper (Family: Lutjanidae) in coastal nurseries. *Coral Reefs* 30:1135–1145
- McMahon KW, Ling Hamady L, Thorrold SR (2013) A review of ecogeochemistry approaches to estimating movements of marine animals. *Limnol Oceanogr* 58: 697–714
- Miller RJ, Page HM (2012) Kelp as a trophic resource for marine suspension feeders: a review of isotope-based evidence. *Mar Biol* 159:1391–1402
- Newsome SD, Etnier MA, Gifford-Gonzalez D, Phillips DL and others (2007) The shifting baseline of northern fur seal ecology in the northeast Pacific Ocean. *Proc Natl Acad Sci USA* 104:9709–9714
- Newsome SD, Fogel ML, Kelly L, del Rio CM (2011) Contributions of direct incorporation from diet and microbial amino acids to protein synthesis in Nile tilapia. *Funct Ecol* 25:1051–1062
- O'Brien DM, Fogel ML, Boggs CL (2002) Renewable and nonrenewable resources: amino acid turnover and allocation to reproduction in Lepidoptera. *Proc Natl Acad Sci USA* 99:4413–4418
- Olive PJW, Pinnegar JK, Polunin NVC, Richards G, Welch R (2003) Isotope trophic-step fractionation: a dynamic equilibrium model. *J Anim Ecol* 72:608–617
- Olson RJ, Popp BN, Graham BS, López-Ibarra GA and others (2010) Food-web inferences of stable isotope spatial patterns in copepods and yellowfin tuna in the pelagic eastern Pacific Ocean. *Prog Oceanogr* 86:124–138
- Page HM, Reed DC, Brzezinski MA, Melack JM, Dugan JE (2008) Assessing the importance of land and marine sources of organic matter to kelp forest food webs. *Mar Ecol Prog Ser* 360:47–62
- Pennington JT, Chavez FP (2000) Seasonal fluctuations of temperature, salinity, nitrate, chlorophyll and primary production at station H3/M1 over 1989–1996 in Monterey Bay, California. *Deep-Sea Res II* 47:947–973
- Peterson BJ, Fry B (1987) Stable isotopes in ecosystem studies. *Annu Rev Ecol Systematics* 18:293–320
- Post DM (2002) Using stable isotopes to estimate trophic position: models, methods, and assumptions. *Ecology* 83: 703–718
- Post DM, Layman CA, Arrington DA, Takimoto G, Quattrochi J, Montaña CG (2007) Getting to the fat of the matter: models, methods and assumptions for dealing with lipids in stable isotope analysis. *Oecologia* 152:179–189
- R Development Core Team (2012) R: a language and environment for statistical computing. R Foundation for Statistical Computing, Vienna
- Rau GH, Sweeney RE, Kaplan IR (1982) Plankton $^{12}\text{C}/^{13}\text{C}$ ratio changes with latitude: differences between northern and southern oceans. *Deep-Sea Res* 29:1035–1039
- Rau GH, McHugh CM, Harrold C, Baxter C, Hecker B, Embley RW (1990) $\delta^{13}\text{C}$, $\delta^{15}\text{N}$ and $\delta^{18}\text{O}$ of *Calyptogena phaseoliformis* (bivalve mollusc) from the Ascension Fan Valley near Monterey, California. *Deep-Sea Res A Oceanogr Res Pap* 37:1669–1676
- Rau GH, Takahashi T, Marais Des DJ, Repeta DJ, Martin JH (1992) The relationship between delta ^{13}C of organic matter and $[(\text{CO}_2)\text{aq}]$ in ocean surface water: data from a JGOFS site in the northeast Atlantic Ocean and a model. *Geochim Cosmochim Acta* 56:1413–1419
- Rau GH, Chavez FP, Friederich GE (2001) Plankton $^{13}\text{C}/^{12}\text{C}$ variations in Monterey Bay, California: evidence of non-diffusive inorganic carbon uptake by phytoplankton in an upwelling environment. *Deep-Sea Res I* 48:79–94
- Ruiz-Cooley RI, Gerrodette T (2012) Tracking large-scale latitudinal patterns of $\delta^{13}\text{C}$ and $\delta^{15}\text{N}$ along the E Pacific using epi-mesopelagic squid as indicators. *Ecosphere* 3: art63
- Scott JH, O'Brien DM, Emerson D, Sun H, McDonald GD, Salgado A, Fogel ML (2006) An examination of the carbon isotope effects associated with amino acid biosynthesis. *Astrobiology* 6:867–880
- Sherwood OA, Heikoop JM, Scott DB, Risk MJ, Guilderson TP, McKinney RA (2005) Stable isotopic composition of deep-sea gorgonian corals *Primnoa* spp.: a new archive of surface processes. *Mar Ecol Prog Ser* 301:135–148
- Silfer JA, Engel MH, Macko SA, Jumeau EJ (1991) Stable carbon isotope analysis of amino-acid enantiomers by conventional isotope ratio mass spectrometry and combined gas-chromatography isotope ratio mass spectrometry. *Anal Chem* 63:370–374
- Simenstad CA, Wissmar RC (1985) $\delta^{13}\text{C}$ evidence of the origins and fates of organic carbon in estuarine and near-shore food webs. *Mar Ecol Prog Ser* 22:141–152
- Simenstad CA, Duggins DO, Quay PD (1993) High turnover of inorganic carbon in kelp habitats as a cause of $\delta^{13}\text{C}$ variability in marine food webs. *Mar Biol* 116:147–160
- Smith BN, Epstein S (1971) Two categories of $^{13}\text{C}/^{12}\text{C}$ ratios for higher plants. *Plant Physiol* 47:380–384
- Somes CJ, Schmittner A, Galbraith ED, Lehmann MF, Altabet MA, Montoya JP (2010) Simulating the global distribution of nitrogen isotopes in the ocean. *Global Biogeochem Cycles* 24:GB4019
- Tallis H (2009) Kelp and rivers subsidize rocky intertidal communities in the Pacific Northwest (USA). *Mar Ecol Prog Ser* 389:85–96
- Vander Zanden MJ, Rasmussen JB (2001) Trophic fractionation: implications for aquatic food web studies. *Limnol Oceanogr* 46:2061–2066
- Venables WN, Ripley BD (2002) Modern applied statistics with S, 4th edn. Springer, New York, NY
- Walker BD, McCarthy MD (2012) Elemental and isotopic characterization of dissolved and particulate organic matter in a unique California upwelling system: importance of size and composition in the export of labile material. *Limnol Oceanogr* 57:1757–1774
- Widdows J, Fieth P, Worrall CM (1979) Relationships between seston, available food and feeding activity in the common mussel *Mytilus edulis*. *Mar Biol* 50:195–207